HHS Public Access

Author manuscript

Nat Med. Author manuscript; available in PMC 2014 August 01.

Published in final edited form as:

Nat Med. 2013 August ; 19(8): 1047–1053. doi:10.1038/nm.3218.

Origin and Function of Myofibroblasts in Kidney Fibrosis

Valerie S. LeBleu[1,2], **Gangadhar Taduri**[2], **Joyce O'Connell**[2], **Yingqi Teng**[2], **Vesselina G. Cooke**[2], **Craig Woda**[2], **Hikaru Sugimoto**[1,2], and **Raghu Kalluri**[1,2,3,4]

[1]Department of Cancer Biology, Metastasis Research Center, University of Texas MD Anderson Cancer Center, Houston, Texas

[2]Division of Matrix Biology, Department of Medicine, Beth Israel Deaconess Medical Center, Boston, MA

[3]Department of Biological Chemistry and Molecular Pharmacology, Harvard Medical School, Boston, MA

[4]Harvard-MIT Division of Health Sciences and Technology, Boston, MA

Abstract

Myofibroblasts are associated with organ fibrosis but their precise origin and functional role remain unknown. We employed multiple genetically engineered mice to track, fate-map and ablate cells to determine the source and function of myofibroblasts in kidney fibrosis. Such comprehensive analysis identified that the total pool of myofibroblasts is split, with 50% arising from local resident fibroblasts via proliferation. The non-proliferating myofibroblasts derive via differentiation from bone marrow (35%), endothelial to mesenchymal transition (EndMT) program (10%) and epithelial to mesenchymal transition (EMT) program (5%). Specific deletion of *Tgfbr2* in αSMA$^+$ cells revealed the importance of this pathway in recruitment of myofibroblasts via differentiation. Using genetic mouse models and fate-mapping strategy we determined that vascular pericytes likely do not contribute to the emergence of myofibroblasts or fibrosis. This study suggests that targeting diverse pathways is required to significantly inhibit composite accumulation of myofibroblasts in kidney fibrosis.

Introduction

Myofibroblasts are considered to be the dominant collagen-producing cells in many pathologies, including wound healing, organ fibrosis, and cancer[1–3]. The speculated role for myofibroblasts in organ fibrosis is diverse and dynamic in the disease progression. In wound healing, the scarring process reverses when repair is accomplished with myofibroblasts disappearing upon resolution of the wound[1]. In the context of organ fibrosis, myofibroblasts

Address for Correspondence: Raghu Kalluri, Professor of Cancer Biology, Department of Cancer Biology, Metastasis Research Center, UT MD Anderson Cancer Center, Houston, TX 77025, rkalluri@MDanderson.org.

Conflict of Interest: None

Author Contributions

RK provided the conceptual framework, intellectual input, designed the study and helped in the writing of the manuscript. VSL designed the study, provided intellectual input, performed experiments, collected data and wrote the manuscript. VSL, GT, YT, VGC, HS, and JTO and CW performed some experiments and collected data. The data was analyzed by VSL, GT, HS and CW.

persist and extracellular matrix (ECM) continues to accumulate due to unabated tissue insult, replacing the functional parenchyma of the organ and contributing to its failure. Despite increased knowledge of immune mediators of fibrosis, which today constitute the only therapeutic targets to manage organ fibrosis in our patients, there is no specific treatment option to control fibrosis and preserve organ function. Effective targeting of myofibroblasts in organ fibrosis remains a challenge due incomplete knowledge regarding their origin and functional contribution.

The origin of resident myofibroblasts during organ development is undisputed due to their presumptive mesodermal origin, however their origin during fibrosis continues to be a subject of intense debate. In this regard, previous studies have suggested a possible role for vascular pericyte-derived myofibroblasts in the pathogenesis of renal fibrosis[4,5], albeit, functional data is still lacking. These studies follow original studies first published in the cancer and developmental biology literature suggesting that pericytes may give rise to myofibroblasts[2,6–8]. Others proposed a role for epithelial to mesenchymal transition[9–12], endothelial to mesenchymal transition[13,14], and bone marrow recruitment[15,16] in the emergence of fibrosis associated myofibroblasts. In order to unequivocally determine the source and function of myofibroblasts in kidney fibrosis, we employed multiple genetic mouse models to track, fate map, and ablate mesenchymal cells. This study informs new therapeutic strategies to control fibrosis.

Result

Myofibroblast derive from resident and bone marrow sources

Using mice that enabled visualization of αSMA$^+$ cells (αSMA-RFP mice) and fate mapping of these cells using the newly generated αSMA promoter driven cre-loxP mediated expression of yellow fluorescent protein mice (αSMACre; YFP$^{f/f}$ mice), we demonstrated that renal fibrosis (following unilateral ureteral obstruction, UUO) is associated with a significant accumulation of αSMA$^+$ myofibroblasts in the interstitium of fibrotic kidneys[17] (Fig. S1a). In healthy kidneys of αSMA-Cre;YFP$^{f/f}$ mice, only rare interstitial cells are visualized (Fig. S1a). While interstitial myofibroblasts accumulate in fibrosis, their origin remains unknown. To address this issue, we performed several tracking and fate mapping experiments using novel genetic mouse models.

To assess the contribution of resident fibroblasts versus bone marrow derived mesenchymal cells towards the total myofibroblast population in kidney fibrosis, we performed bone marrow transplant experiments using αSMA-RFP mice[17] and wild type (WT) mice. We confirmed that total body irradiation associated with bone marrow transplantation prior to UUO did not impact fibrotic disease progression in our studies (Fig. S1b), and confirmed high bone marrow chimerism in sex-mismatched transplant (~96% chimerism, Fig. S1c). Wild type mice were transplanted with bone marrow from αSMA-RFP donor mice and a reverse transplant (αSMA-RFP mice transplanted with bone marrow from WT donor) was also performed, followed by induction of renal fibrosis. Immunolabeling for αSMA$^+$ cells (green) and visualization of αSMA-RFP$^+$ cells (red) indicated that in the fibrotic kidneys of the transplanted mice about 35% of αSMA$^+$ myofibroblasts were bone marrow derived,

whereas about 65% of αSMA$^+$ cells were derived from expansion of resident cells or other sources than bone marrow (Fig. 1a–b).

Next, we evaluated the proliferation status of myofibroblasts in kidney fibrosis. In αSMA-RFP mice with fibrosis, about 50% of the myofibroblasts was labeled for the proliferation marker Ki67 (Fig. 1c–d). These studies suggested that 50% of the myofibroblasts are recruited without a need for expansion via proliferation. Our bone marrow transplant studies revealed that all the bone marrow derived fibroblasts do not label for proliferation markers (Fig. S1d–e), suggesting that recruitment of bone marrow derived myofibroblasts occurs without proliferation.

Myofibroblasts are functionally important for renal fibrosis

To address the functional importance of myofibroblasts in fibrosis, we generated mice in which viral thymidine kinase (αSMA-tk) was expressed under the control of αSMA promoter. This strategy allowed for the specific ablation of proliferating αSMA$^+$ cells in fibrosis, without an impact on quiescent/non proliferating cells. We treated αSMA-tk mice and wild type (WT) littermate mice with daily i.p. injections of ganciclovir (GCV) following UUO. The mice were euthanized 10 days later and αSMA$^+$ myofibroblasts evaluated by immunostaining. Double immunofluorescence for αSMA and Ki67 in kidneys of αSMA-tk mice treated with GCV (αSMA-tk+GCV) revealed that all proliferating myofibroblasts (locally derived; vide supra) were targeted for ablation, resulting in around 50% reduction in the number of interstitial myofibroblasts (Fig. 1c–d). Together with our bone marrow transplant studies (Fig. 1a and Fig. S1d), these results suggest that out of the 65% of total myofibroblasts that are derived from local sources, about 15% emerged without proliferation.

The ratio of proliferating αSMA$^+$ cells versus non proliferating cells on day 2, day 5 and day 10 post induction of kidney fibrosis remained constant (Fig. 1e), suggesting a linear pattern of myofibroblast accumulation via proliferation of resident αSMA$^+$ cells. Immunohistochemistry analyses of normal kidneys revealed αSMA$^+$ cells in large vessel walls, likely smooth muscle cells, as well as occasional rare interstitial αSMA$^+$ cells (Fig. 1f). Quantitative measurements of immunohistochemistry staining revealed about 50% reduction in interstitial αSMA$^+$ cells following UUO in αSMA-tk+GCV mice compared to control mice (Fig. 1f), similar to the immunofluoresence studies (Fig. 1c–d). The specific ablation of all proliferating myofibroblasts reduced UUO-induced fibrosis, as evidenced by a significant decrease in Masson Trichrome Staining (MTS) (Fig. 1g), Sirius Red staining (Fig. S2a), and type I collagen levels (Fig. S2b–c). All parameters indicated a 50%–60% quantitative reduction in kidney fibrosis following depletion of proliferating αSMA$^+$ myofibroblasts. Similar results were also noted in a genetic model of renal disease fibrosis. We crossed the αSMA-tk mice with the *Col4a3* knockout mice (*Col4a3*$^{-/-}$ mice[18]). Onset of renal disease is observed starting at 8 weeks of age in these mice[18,19], at which point the mice received daily i.p. injections of ganciclovir for 4-weeks. When compared to *Col4a3*$^{-/-}$ control littermate, ablation of ~50% of αSMA$^+$ cells resulted in ~50% reduction in fibrosis (Fig. S3a–b). Despite reduction in fibrosis and αSMA$^+$ myofibroblasts in αSMA-tk+GCV mice, macrophage infiltration (F4/80$^+$ and CD11b$^+$ cells) remained unchanged when

compared to control mice (Fig. S2d–e). While changes in blood pressure were not evaluated, endothelial cell number ($CD34^+$ cells) also remained unchanged in αSMA-tk+GCV mice when compared to GCV treated wild type control mice (Fig. S2f).

Next, sub-lethally irradiated αSMA-tk mice were transplanted with bone marrow from donor αSMA-RFP mice and subjected to UUO. Additionally, a reverse bone marrow transplant was also performed (αSMA-RFP mice were transplanted with αSMA-tk bone marrow). Both sets of mice were administered GCV to ablate proliferating fibroblasts. In the GCV treated αSMA-tk mice transplanted with αSMA-RFP bone marrow, proliferating αSMA ($FITC^+$) myofibroblasts were not detected and the total $αSMA^+$ cells population was reduced by half, while the number of bone marrow derived myofibroblasts was unchanged (Fig. 2a), supporting the notion that recruitment from bone marrow does not require proliferation. Taken together with data from un-transplanted mice, these results indicate that bone marrow derived myofibroblasts were not ablated in αSMA-tk+GCV mice (Fig. 1c–d). Reciprocally, in the GCV treated αSMA-RFP mice transplanted with αSMA-tk bone marrow, the emergence of proliferating $αSMA\text{-}RFP^+$ myofibroblasts and bone marrow derived myofibroblasts was unaffected, confirming that accumulation of $αSMA^+$ myofibroblasts from the bone marrow does not require proliferation. The quantitation of MTS staining indicated a similar reduction in fibrosis in αSMA-tk mice and αSMA-tk mice with αSMA-RFP BMT, while fibrotic index in αSMA-RFP mice with αSMA-tk BMT was similar to control $αSMA\text{-}tk^-$ (WT) mice treated with GCV (Fig. 2b–c). Taken together, the results suggest that expansion of resident cells as well as recruitment of bone marrow-derived cells are functional contributors to kidney fibrosis.

MSCs may contribute to myofibroblasts recruitment

Undifferentiated bone marrow-derived mesenchymal stem cells (MSCs) from αSMA-RFP mice express low levels of αSMA (Fig. 3a–c) and undetectable RFP expression (Fig. 3a–b). TGFβ1 is an important cytokine implicated in the activation of myofibroblasts[20]. While type I collagen gene expression was not detected in MSCs and MSCs treated with TGFβ1 (data not shown), suggesting a longer exposure and additional factors are necessary to induce the expression of matrix protein such as type I collagen in these cells, TGFβ1 induced a partial myofibroblast phenotype in MSCs with robust induction of αSMA expression, supporting the notion that MSCs may give rise to myofibroblasts in renal fibrosis via TGFβ1 dependent differentiation (Fig. 3a–c).

To further validate this notion, we crossed the αSMA-Cre mice with mice harboring floxed allele of TGF-beta type II receptor gene ($Tgfbr2^{f/f}$)[21]. These mice were born in expected Mendelian ratios with no obvious developmental defects. They were viable and fertile in adulthood and present no obvious phenotype or altered life span. Tgfbr2 mediated signaling in $αSMA^+$ cells thus appears nonessential for normal mouse development or its loss is compensated by other pathways. We isolated MSCs from the bone marrow of these mice and subjected them to TGFβ1 treatment (*vide supra*). Loss of *Tgfbr2* prevented MSCs from sustaining a TGFβ1 induced αSMA expression and conversion to myofibroblasts when compared to control cells (Fig. 3d–e), further supporting the notion that TGFβ1 may play a role in differentiation of MSCs into myofibroblasts in kidney fibrosis.

Next, we performed UUO in the αSMA-Cre;*Tgfbr2*$^{f/f}$ mice. Diminished immunolabeling for phosphorylated Smad2 suggested potential attenuation of TGFβ1-mediated signaling in αSMA$^+$ cells in the kidneys of αSMA-Cre;*Tgfbr2*$^{f/f}$ mice when compared to littermate control mice (Fig. S4a). Compared to control mice with fibrosis, about 56% reduction in myofibroblasts was observed in the αSMA-Cre;*Tgfbr2*$^{f/f}$ with fibrosis (Fig. 3f–g). The decrease was restricted predominantly to the non-proliferating myofibroblasts with number of proliferating myofibroblasts largely unchanged (Fig. 3f). Despite 56% reduction in myofibroblasts in these mice, fibrosis was reduced by only about 29% when compared to control littermate mice and tubular atrophy was mildly reduced in αSMA-Cre;*Tgfbr2*$^{f/f}$ (Fig. 3g). The F4/80$^+$ and CD11b$^+$ macrophage recruitment was significantly reduced in the αSMA-Cre;*Tgfbr2*$^{f/f}$ mice with fibrosis (Fig. 3h and Fig. S4b). These results suggest that deletion of *Tgfbr2* in αSMA$^+$ cells specifically impacts the recruitment of myofibroblasts derived via differentiation. A decrease in macrophage number suggests that myofibroblasts that arise via *Tgfbr2* mediated differentiation may help recruit these cells in fibrosis.

NG2$^+$ and PDGFRβ$^+$ pericytes increase in kidney fibrosis

To address the role of pericytes in kidney fibrosis, we generated mice in which the yellow fluorescent protein, cre-recombinase and viral thymidine kinase genes are expressed under the control of *Cspg4* gene promoter (*Cspg4* is therein referred to as NG2–its more commonly used synonym, and mice are referred to as NG2-YFP, NG2-Cre and NG2-tk respectively). *Cspg4* – or NG2, is a cell surface chondroitin sulfate proteoglycan identified as a maker for vascular pericytes[22–24]. Similarly, we used mice in which the red fluorescent protein, cre recombinase and viral thymidine kinase are expressed under the control of the *Pdgfrb* gene promoter (*Pdgfrb*-RFP, *Pdgfrb*-Cre and *Pdgfrb*-tk respectively), another extensively used marker for pericytes[23–30]. The NG2-YFP$^+$ and *Pdgfrb*-RFP$^+$ cells were detected in association with CD31$^+$ endothelial cells, suggesting that pericytes are labeled efficiently in these mice (NG2-YFP and *Pdgfrb*-RFP mice) (Fig. S4c–d).

YFP visualization showed a significant accumulation in NG2$^+$ interstitial cells in UUO-induced renal fibrosis, whereas such labeling was rarely observed in the interstitium of the healthy kidneys (Fig. 4a). The number of interstitial Pdgfrb$^+$ cells also significantly increased following UUO-induced fibrosis (Fig. 4b). The observed interstitial expansion of NG2$^+$ and Pdgfrb$^+$ cells in fibrotic kidneys of the transgenic mice was further confirmed using antibody labelling strategies (Fig. 4c–d).

Pericytes do not contribute to kidney fibrosis

A similar approach as described using the αSMA-tk mice was employed to address the functional role of NG2$^+$ cells in UUO-induced renal fibrosis. NG2-tk and WT littermate mice were treated with daily i.p. injection of GCV following UUO, and the mice were euthanized 10 days later. Quantitative analytic measurements of immunolabeled kidney sections revealed approximately 55% reduction in interstitial NG2$^+$ cells following UUO in NG2-tk mice compared to WT littermate controls (Fig. 4c). Similar results were also noted when *Col4a3* knockout mice (a genetic mouse model of kidney disease and fibrosis; *Col4a3*$^{-/-}$) crossed with NG2-tk mice (*Col4a3*$^{-/-}$;NG2-tk mice) were subjected to GCV treatment leading to the ablation of proliferating NG2$^+$ cells (Fig. S3c–d).

Similarly, *Pdgfrb*-tk and WT littermate mice were treated with daily i.p. injection of GCV following UUO, and the mice were euthanized 10 days later. Quantitative analytic measurements of immunolabeled kidney sections revealed approximately 80% reduction in interstitial Pdgfrb$^+$ cells following UUO in *Pdgfrb*tk compared to WT littermate control (Fig. 4d). Renal fibrosis was assessed using MTS, Sirius red staining, and type I collagen immunolabeling and gene expression measurements. All parameters indicated insignificant reduction in fibrosis following depletion of NG2$^+$ cells or Pdgfrb$^+$ cells (Fig. 4e, Fig. S2c and Fig. S5a–d), suggesting that these cells may not contribute to fibrosis. Macrophage infiltration was unchanged in the pericytes depleted fibrotic kidneys (Fig. S5e–f). We next employed fate-mapping experiments to address whether αSMA$^+$ myofibroblasts emerge from vascular pericytes in renal fibrosis. Immunolabeling of αSMA$^+$ cells in NG2-Cre;YFP$^{f/f}$ reporter mice revealed on average 3% overlap, thus indicating that the majority of αSMA$^+$ cells did not derive from NG2$^+$ cells (Fig. S6a–b). Interestingly, Pdgfrb immunolabeling revealed around 35% overlap with NG2-Cre;YFP positive cells, indicating that a subset of Pdgfrb$^+$ interstitial cells share a common lineage with NG2$^+$ vascular pericytes (data not shown). A similar strategy using *Pdgfrb*-Cre;YFP$^{f/f}$ reporter mice, and co-immunolabeling with αSMA$^+$ cells revealed on average 6% overlap (Fig. S6c–d). These results suggest that αSMA$^+$ cells predominantly do not emerge from Pdgfrb$^+$ cells.

To further confirm that our ablation studies specifically deleted αSMA$^+$ cells without altering the numbers of NG2$^+$ and Pdgfrb$^+$ cells in renal fibrosis, we surveyed fibrotic kidneys of αSMA-tk mice treated with GCV for NG2$^+$ and Pdgfrb$^+$ cells. Both NG2$^+$ and Pdgfrb$^+$ cells remained unaltered in their number in the GCV treated αSMA-tk mice when compared to control fibrotic kidneys (Fig. S6e–f), indicating specific targeting of NG2$^-$/αSMA$^+$ and Pdgfrb$^-$/αSMA$^+$ cells. Similar experiments were performed using kidneys from NG2-tk and *Pdgfrb*-tk mice treated with GCV. The number of αSMA$^+$ cells remained the same in both NG2-tk and *Pdgfrb*-tk mice treated with GCV despite significant reduction in NG2$^+$ and Pdgfrb$^+$ cells, respectively (Fig. S6g–h).

EMT and EndMT contribution to myofibroblasts

Epithelial to mesenchymal transition (EMT) has been proposed as source for myofibroblasts in the kidney and has been disputed by others[31,32]. Inhibition of EMT program improves renal fibrosis[33]. Using compound transgenic mice, we revisited the epithelial-to-mesenchymal (EMT) program as a source of myofibroblasts. We generated mice in which γGT-Cre driven cre-loxP mediated expression of yellow fluorescent protein (γGT-Cre;YFP$^{f/f}$ mice). In the kidney, γGT expression is detected in tubular epithelial cells[9,33]. These mice were subsequently crossed with αSMA-RFP to generate γGT-Cre;YFP$^{f/f}$;αSMA-RFP mice and subjected to UUO induced fibrosis. Visualization of the fluorescent signals indicated that significant number of tubular cells express RFP, with increasing number of double positive tubules with progression of fibrosis. However, a very small number of interstitial αSMA$^+$ myofibroblasts arose from fully executed EMT, accounting for approximately 5% of the total interstitial αSMA$^+$ myofibroblasts (Fig. 5a–e).

We also generated mice to visualize interstitial αSMA$^+$ cells derived from the vascular endothelium. *Cdh5*-Cre mice were crossed to obtain *Cdh5*-Cre;YPF$^{f/f}$;αSMA-RFP mice to

fate map (via cre-loxP mediated expression of YFP) the contribution of endothelial cells to the accumulation of myofibroblasts (Fig. 5f). Vessels were YFP$^+$ in the healthy kidney (Fig. 5f). Visual inspection of the fibrotic kidney subjected to UUO showed that approximately 10% of interstitial myofibroblasts co-localized with markers of vessel associated endothelial cells (YFP) and αSMA-RFP (red) (Fig. 5f–g).

Discussion

Many different investigators have proposed a central role for myofibroblasts in kidney fibrosis but functional validation was not attempted until this study. Using newly generated genetic mouse models, we were able to demonstrate that myofibroblasts are functional contributor of type I collagen production and kidney fibrosis. The origin of myofibroblasts has been an intense source of debate in the recent years with diverse proposals for their origin. Some studies have disputed the contribution of EMT in the emergence of myofibroblasts and fibrosis[31], while other favor the idea that vascular pericytes serve as precursors of myofibroblasts in fibrosis[4,5], based on earlier experiments published in the cancer and development biology literature which suggested pericytes as a source for putative myofibroblasts[2,6–8,34]. Many recent studies have also proposed a contribution of endothelial to mesenchymal transition (EndMT) in the generation of myofibroblasts[14,35,36]. A suggestion that bone marrow contributes to the total myofibroblast population was also put forward[15,16]. Due to such diverse opinions about the origin of myofibroblasts in fibrosis, we performed a comprehensive study to address all possible sources of myofibroblasts in kidney fibrosis.

Our results revealed that accumulation of myofibroblasts occurs predominantly from two different sources. One involves local proliferation of resident tissue fibroblasts (about 50%), and the other (35%) involves contribution of bone marrow-derived cells without any evidence of proliferation in the kidney. We show that bone marrow derived mesenchymal stem cells (MSC) can differentiate into myofibroblasts under the influence of TGFβ1 and their potential recruitment of bone marrow is dependent on the expression of *Tgfbr2*. The loss of *Tgfbr2* in αSMA$^+$ cells lead to approximately 56% reduction in the accumulation of myofibroblasts but resulted in only about 29% reduction in fibrosis. Apart from myofibroblasts derived via proliferation of local resident fibroblasts, all other sources of myofibroblast accumulation that occurs via differentiation (bone marrow, EMT and EndMT) appeared to be affected by the loss of *Tgfbr2*. Collectively, these results highlight a couple of possibilities. One, bone marrow-derived and EMT/EndMT-derived myofibroblasts may not contribute to the predominant amount of type I collagen accumulation observed in fibrosis, supporting some previous observations[4,5]. Two, because ablation of proliferating myofibroblasts led to 50% reduction in fibrosis, the possibility that other (non-myofibroblasts) type I collagen producing cells exist in kidney fibrosis cannot be ruled out. Future experiments will likely shed more light on this matter.

Conversion of local resident fibroblasts into myofibroblasts involves proliferation, while recruitment of bone marrow derived myofibroblasts is independent of proliferation and rather relies on migration and differentiation. These findings immediately inform the clinic that anti-proliferative drugs can only partially impact the total myofibroblast accumulation

in the fibrotic kidney. This study provides new insight into the contribution of bone marrow to type I collagen producing- and scar-forming myofibroblasts. The *Tgfbr2* deletion experiments suggest that pre-clinical studies targeting TGFβ1 or its receptor/s may result in sub-optimal responses due to diverse origin and mechanisms for myofibroblast accumulation.

Using genetic mouse model that specifically track, fate map and delete pericytes, we demonstrate that $NG2^+$ pericytes and $PDGFR\beta^+$ pericytes do not contribute to the myofibroblast population in kidney fibrosis. This was also recently noted in a lung fibrosis model[37]. Additionally, we show that specific deletion of pericytes does not improve kidney fibrosis nor alter the recruitment of myofibroblasts. These results are opposite to studies reported by others using the same UUO kidney fibrosis model[4,5]. There are many possible explanations for this discrepancy. First, the mice used (Coll1a1-GFP and FoxD1) to track pericytes by Humphreys/Lin and colleagues[4,5] may not be specific for pericytes[7]. Second, type I collagen is made by many cell types in the context of fibrosis, including epithelial cells, endothelial cells and several types of mesenchymal cells, and thus the use of Coll1a1-GFP mice to track pericytes may have led to confusing results. Third, the use of FoxD1 mice does not substitute for the use of *Pdgfrb* and NG2 promoter driven mice, the accepted pericytes markers[7]. Fourth, antibody labeling can be subjective, while use of pericytes fate-mapping mice combined with immunolabeling strategies is more informative.

This study confirms previous reports that EMT program does not lead to the generation of a significant number of interstitial myofibroblasts in fibrosis[4.5,34]. Our fate mapping experiments show that while a significant number of tubular epithelial cells gain αSMA expression in fibrosis, only about 5% of myofibroblasts are truly derived via a fully executed EMT. We also confirm that about 10% of myofibroblasts are derived via EndMT.

In summary, our comprehensive and functional audit of myofibroblast origin in kidney fibrosis reveals that about half of the myofibroblasts emerge via proliferation and the rest are recruited via differentiation. Local fibroblast expansion contributes to about 50% to the myofibroblast pool, while about 35% are recruited from the bone marrow. EndMT contributes to about 10% and EMT program generates about 5% of interstitial myofibroblasts and both EndMT and EMT likely involve TGFβ1 dependent-differentiation[11,12,14,38]. While this information is derived using kidney fibrosis as a model system, we believe that it serves as an important baseline for future fibrosis studies with other organs. This study also informs new therapy targets for kidney fibrosis, which is urgently needed in the clinic.

Supplementary Material

Refer to Web version on PubMed Central for supplementary material.

Acknowledgements

This study was supported by US National Institutes of Health Grants DK55001, DK81976, CA125550, CA155370 and CA151925. R. Kalluri is supported by the Cancer Prevention and Research Institute of Texas, Metastasis Research Center at MD Anderson Cancer Center. V. LeBleu was funded by the US National Institutes of Health Research Training Grant in Gastroenterology (2T32DK007760-11), V. Cooke was funded by US National Research

Service Award (NRSA) F32 Ruth Kirschstein Post-doctoral Fellowship from the US National Institutes of Health (5F32DK082119-02), H. Sugimoto was funded by the US National Institutes of Health Research Training Grant in Cardiovascular Biology (5T32HL007374-30), J. O'Connell was funded by the US Department of Defense Breast Cancer Research Predoctoral Traineeship Award (W81XWH-09- 1-0008), G. Taduri was funded by the International Society of Nephrology Fellowship, and C. Woda was funded by the US National Institutes of Health Research Training Grant in Pediatric Nephrology (T32DK007726). *Pdgfrb*-Cre mice were kindly provided by R. Adams, Max Planck Institute for Molecular Biomedicine, Münster, Germany. γGT-Cre mice were kindly provided by E. Neilson, Northwestern University, Chicago, IL. *Tgfbr2*$^{f/f}$ mice were kindly provided by H. Moses, Vanderbilt University, Nashville, TN.

References

1. Gabbiani G. The myofibroblast in wound healing and fibrocontractive diseases. The Journal of pathology. 2003; 200:500–503. [PubMed: 12845617]
2. Sugimoto H, Mundel TM, Kieran MW, Kalluri R. Identification of fibroblast heterogeneity in the tumor microenvironment. Cancer Biol Ther. 2006; 5:1640–1646. [PubMed: 17106243]
3. Meran S, Steadman R. Fibroblasts and myofibroblasts in renal fibrosis. Int J Exp Pathol. 2011; 92:158–167. [PubMed: 21355940]
4. Humphreys BD, et al. Fate tracing reveals the pericyte and not epithelial origin of myofibroblasts in kidney fibrosis. The American journal of pathology. 2010; 176:85–97. [PubMed: 20008127]
5. Lin SL, Kisseleva T, Brenner DA, Duffield JS. Pericytes and perivascular fibroblasts are the primary source of collagen-producing cells in obstructive fibrosis of the kidney. The American journal of pathology. 2008; 173:1617–1627. [PubMed: 19008372]
6. Ronnov-Jessen L, Petersen OW, Koteliansky VE, Bissell MJ. The origin of the myofibroblasts in breast cancer. Recapitulation of tumor environment in culture unravels diversity and implicates converted fibroblasts and recruited smooth muscle cells. J Clin Invest. 1995; 95:859–873. [PubMed: 7532191]
7. Armulik A, Genove G, Betsholtz C. Pericytes: developmental, physiological, and pathological perspectives, problems, and promises. Dev Cell. 2011; 21:193–215. [PubMed: 21839917]
8. Hall AP. Review of the pericyte during angiogenesis and its role in cancer and diabetic retinopathy. Toxicol Pathol. 2006; 34:763–775. [PubMed: 17162534]
9. Iwano M, et al. Evidence that fibroblasts derive from epithelium during tissue fibrosis. J Clin Invest. 2002; 110:341–350. [PubMed: 12163453]
10. Kalluri R, Neilson EG. Epithelial-mesenchymal transition and its implications for fibrosis. J Clin Invest. 2003; 112:1776–1784. [PubMed: 14679171]
11. Zeisberg M, Kalluri R. Fibroblasts emerge via epithelial-mesenchymal transition in chronic kidney fibrosis. Front Biosci. 2008; 13:6991–6998. [PubMed: 18508710]
12. Zeisberg M, Kalluri R. The role of epithelial-to-mesenchymal transition in renal fibrosis. J Mol Med. 2004; 82:175–181. [PubMed: 14752606]
13. Li J, Qu X, Bertram JF. Endothelial-myofibroblast transition contributes to the early development of diabetic renal interstitial fibrosis in streptozotocin-induced diabetic mice. The American journal of pathology. 2009; 175:1380–1388. [PubMed: 19729486]
14. Zeisberg EM, Potenta SE, Sugimoto H, Zeisberg M, Kalluri R. Fibroblasts in kidney fibrosis emerge via endothelial-to-mesenchymal transition. J Am Soc Nephrol. 2008; 19:2282–2287. [PubMed: 18987304]
15. Broekema M, et al. Bone marrow-derived myofibroblasts contribute to the renal interstitial myofibroblast population and produce procollagen I after ischemia/reperfusion in rats. J Am Soc Nephrol. 2007; 18:165–175. [PubMed: 17135399]
16. Li J, Deane JA, Campanale NV, Bertram JF, Ricardo SD. The contribution of bone marrow-derived cells to the development of renal interstitial fibrosis. Stem cells (Dayton, Ohio). 2007; 25:697–706.
17. Lebleu VS, et al. Identification of human epididymis protein-4 as a fibroblastderived mediator of fibrosis. Nature medicine. 2013; 19:227–231.
18. Lebleu V, et al. Stem Cell Therapies Benefit Alport Syndrome. J Am Soc Nephrol. 2009

19. LeBleu V, Sugimoto H, Miller CA, Gattone VH II, Kalluri R. Lymphocytes are Dispensable for Glomerulonephritis but Required for Renal Interstitial Fibrosis in Matrix Defect Induced Alport Renal Disease. Laboratory Investigation. 2008; 88:284–292. [PubMed: 18180701]
20. Leask A, Abraham DJ. TGF-beta signaling and the fibrotic response. Faseb J. 2004; 18:816–827. [PubMed: 15117886]
21. Chytil A, Magnuson MA, Wright CV, Moses HL. Conditional inactivation of the TGF-beta type II receptor using Cre:Lox. Genesis. 2002; 32:73–75. [PubMed: 11857781]
22. Ozerdem U, Grako KA, Dahlin-Huppe K, Monosov E, Stallcup WB. NG2 proteoglycan is expressed exclusively by mural cells during vascular morphogenesis. Dev Dyn. 2001; 222:218–227. [PubMed: 11668599]
23. Bergers G, Song S. The role of pericytes in blood-vessel formation and maintenance. Neuro Oncol. 2005; 7:452–464. [PubMed: 16212810]
24. Cooke VG, et al. Pericyte depletion results in hypoxia-associated epithelial-tomesenchymal transition and metastasis mediated by met signaling pathway. Cancer Cell. 2012; 21:66–81. [PubMed: 22264789]
25. Diaz-Flores L, et al. Pericytes. Morphofunction, interactions and pathology in a quiescent and activated mesenchymal cell niche. Histol Histopathol. 2009; 24:909–969. [PubMed: 19475537]
26. Hirschi KK, D'Amore PA. Pericytes in the microvasculature. Cardiovasc Res. 1996; 32:687–698. [PubMed: 8915187]
27. Lindahl P, Johansson BR, Leveen P, Betsholtz C. Pericyte loss and microaneurysm formation in PDGF-B-deficient mice. Science. 1997; 277:242–245. [PubMed: 9211853]
28. Song S, Ewald AJ, Stallcup W, Werb Z, Bergers G. PDGFRbeta+ perivascular progenitor cells in tumours regulate pericyte differentiation and vascular survival. Nat Cell Biol. 2005; 7:870–879. [PubMed: 16113679]
29. Foo SS, et al. Ephrin-B2 controls cell motility and adhesion during blood-vesselwall assembly. Cell. 2006; 124:161–173. [PubMed: 16413489]
30. Abraham S, Kogata N, Fassler R, Adams RH. Integrin beta1 subunit controls mural cell adhesion, spreading, and blood vessel wall stability. Circ Res. 2008; 102:562–570. [PubMed: 18202311]
31. Kriz W, Kaissling B, Le Hir M. Epithelial-mesenchymal transition (EMT) in kidney fibrosis: fact or fantasy? J Clin Invest. 2011; 121:468–474. [PubMed: 21370523]
32. Liu Y. New Insights into Epithelial-Mesenchyal Transition in Kidney Fibrosis. JASN. 2011; 21:212–222. [PubMed: 20019167]
33. Sugimoto H, et al. Activin-like kinase 3 is important for kidney regeneration and reversal of fibrosis. Nat Med. 2012; 18:396–404. [PubMed: 22306733]
34. Collett GD, Canfield AE. Angiogenesis and pericytes in the initiation of ectopic calcification. Circ Res. 2005; 96:930–938. [PubMed: 15890980]
35. Hashimoto N, et al. Endothelial-mesenchymal transition in bleomycin-induced pulmonary fibrosis. Am J Respir Cell Mol Biol. 2010; 43:161–172. [PubMed: 19767450]
36. Zeisberg EM, et al. Endothelial-to-mesenchymal transition contributes to cardiac fibrosis. Nature medicine. 2007; 13:952–961.
37. Rock JR, et al. Multiple stromal populations contribute to pulmonary fibrosis without evidence for epithelial to mesenchymal transition. Proceedings of the National Academy of Sciences of the United States of America. 2011; 108:E1475–E1483. [PubMed: 22123957]
38. Zeisberg M, et al. BMP-7 counteracts TGF-beta1-induced epithelial-tomesenchymal transition and reverses chronic renal injury. Nature medicine. 2003; 9:964–968.

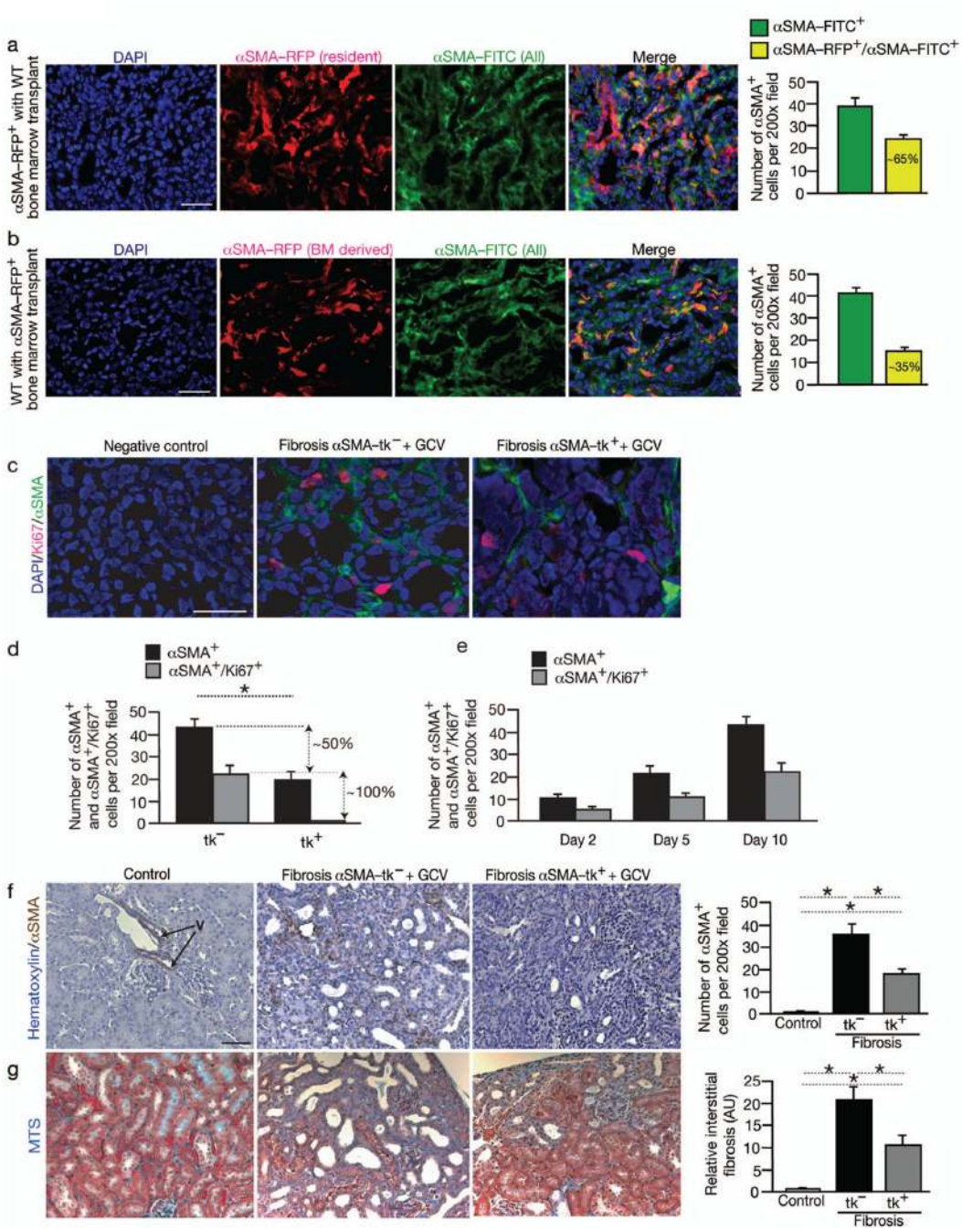

Fig. 1. αSMA$^+$ myofibroblasts derive from resident tissue cells and bone marrow and functionally contribute to renal fibrosis

(**a**) Immunolabeling for total αSMA$^+$ population (αSMA-FITC$^+$ or green) of fibrotic kidney of αSMA-RFP mice transplanted with bone marrow from wild type (WT) donor (n = 5). Graph depicts the number of all αSMA$^+$ cells (αSMA-FITC$^+$ or green) and αSMA$^+$ cells from recipient (resident) (αSMA-FITC$^+$/αSMA-RFP$^+$). Relative percentage is listed. (**b**) Immunolabeling for total αSMA$^+$ population (αSMA-FITC$^+$ or green) of fibrotic kidney of WT mice transplanted with bone marrow from αSMA-RFP donor (n = 5). Graph depicts the

number of all αSMA$^+$ cells (αSMA-FITC$^+$ or green) and αSMA$^+$ cells from bone marrow (αSMAFITC$^+$/ αSMA-RFP$^+$). Relative percentage is listed. (**c**) Immunolabeling for αSMA and Ki67 in fibrotic kidney of αSMA-tk– control mice (n = 5) and αSMA-tk$^+$ mice (n = 5) treated with GCV at day 10 post UUO and (**d**) quantitation of αSMA$^+$/Ki67$^+$ myofibroblasts. Negative control: secondary antibody only. (**e**) Quantitation of αSMA$^+$/Ki67$^+$ myofibroblasts in fibrotic kidney 2 days (n = 5) and 5 days (n = 5) post UUO. (**f**) Immunohistochemistry labeling and quantitative analyses for αSMA in healthy contralateral (Control, n = 5) and fibrotic kidneys from litter mate wild type (αSMA-tk$^-$) (n = 5) and αSMA-tk$^+$ mice (n = 5) treated with ganciclovir (GCV). Arrows point to vessel: 'V'. (**g**) Representative Masson Trichrome staining (MTS) and morphometric analysis for relative interstitial fibrosis of indicated experimental groups (Control: healthy contralateral, tk$^-$: αSMA-tk$^-$, and tk$^+$ αSMA-tk$^+$; all treated with GCV). AU: Arbitrary Units. DAPI(blue): nuclei. Scale bar: 50 μm. Data is presented as mean ± s.e.m. t-test, *P < 0.05.

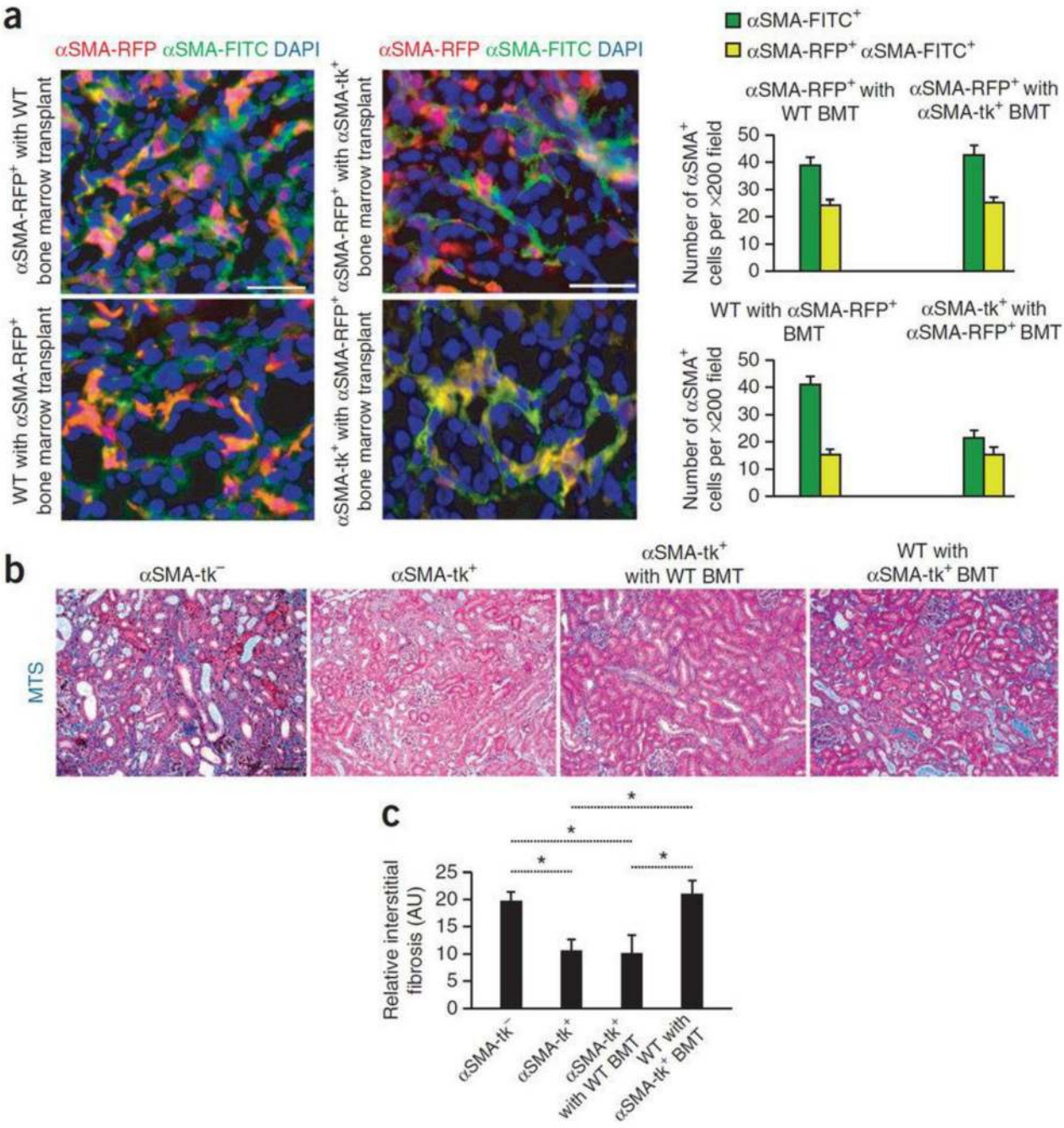

Fig. 2. Bone marrow derived myofibroblasts contribute to fibrosis and emerge independently from proliferation

(**a**) Immunolabeling for all αSMA$^+$ cells (αSMA-FITC$^+$) of fibrotic kidney of indicated experimental groups. Graph depicts the number of all αSMA$^+$ cells (αSMA-FITC$^+$) and αSMA-RFP$^+$/αSMA-FITC$^+$ cells from either bone marrow or resident, depending on host/donor transplantation group (in each group $n = 5$). Left panels are insets from Fig. 1a–b. (**b**) Representative Masson Trichrome staining (MTS) of littermate wild type (WT) control (αSMA-tk$^-$, $n = 5$), αSMA-tk$^+$ ($n = 5$), αSMA-tk$^+$ with WT bone marrow transplant (BMT)

($n = 5$), and WT with αSMA-tk$^+$ BMT fibrotic kidneys treated with GCV ($n = 5$). (**c**) Morphometric analysis for relative interstitial fibrosis in indicated experimental groups. AU: Arbitrary Units. DAPI (blue): nuclei. Scale bar: 50 μm. Data is presented as mean ± s.e.m. *t*-test, $^*P < 0.05$.

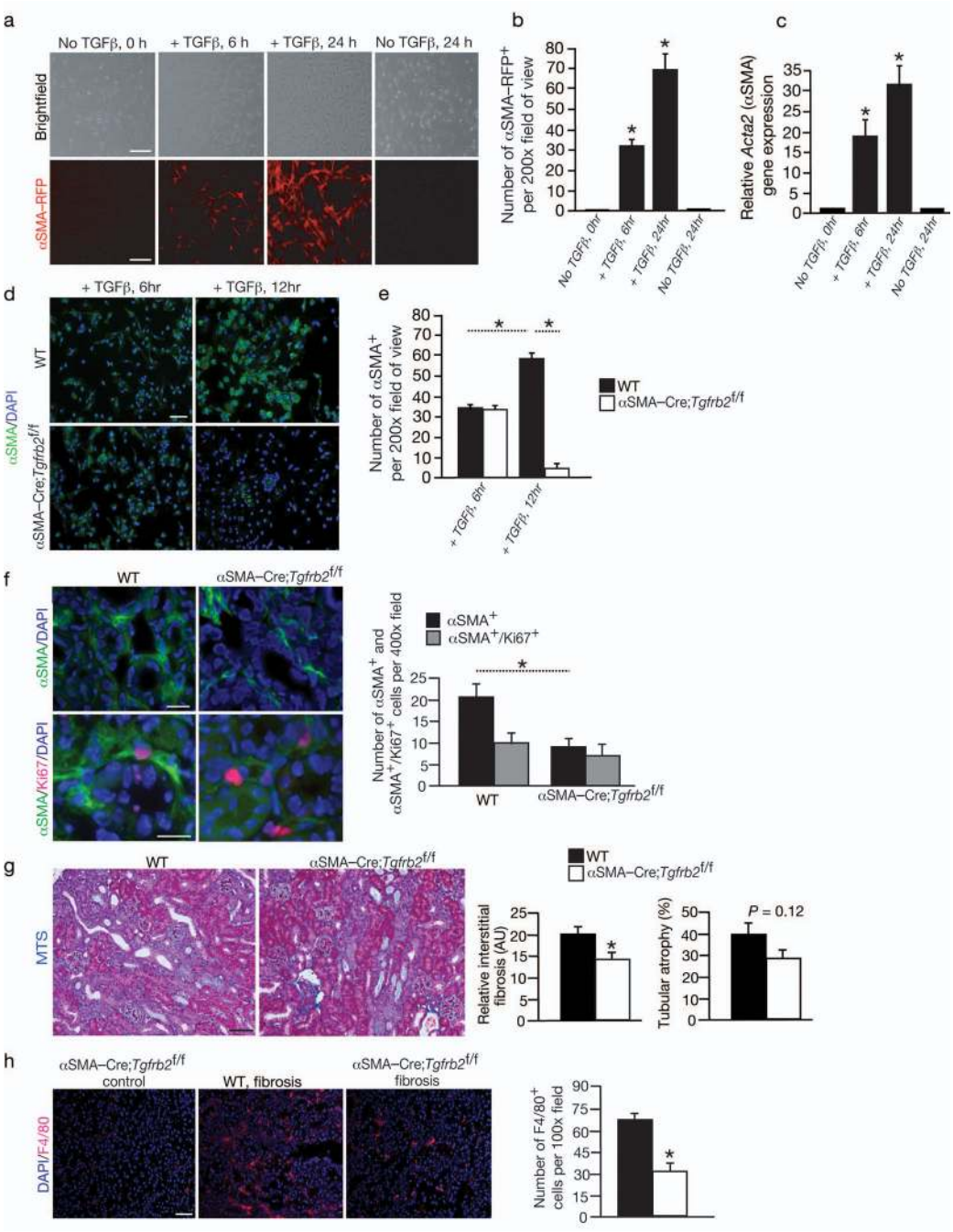

Fig. 3. Bone marrow derived cells differentiate into αSMA$^+$ myofibroblasts in fibrosis via *Tgfbr2* signaling pathway

(**a**). Brightfield and RFP imaging of MSCs from αSMA-RFP mice (n = 3) treated with TGFβ1 and (**b**) quantitation of the number of αSMA-RFP$^+$ cells per visual fields. (**c**) Relative *Acta2* (αSMA) expression by Q-PCR analysis in bone marrow derived mesenchymal stem cells (MSCs) cultured with and without TGFβ1 stimulation. (**d**) αSMA-FITC labeling of MSCs from littermate control WT (n = 3) and αSMA-Cre;*Tgfbr2*$^{f/f}$ mice (n = 3) treated with TGFβ1 at the indicated time and (**e**) quantitation of the number of αSMA$^+$

cells per visual fields. (**f**) Immunolabeling for αSMA and Ki67 in fibrotic kidney of WT (n = 5) and αSMACre; *Tgfbr2*$^{f/f}$ mice (n = 4) and quantitation of αSMA^{+} and αSMA^{+}/Ki67^{+} myofibroblasts. (**g**) Representative Masson Trichrome staining (MTS) of WT and αSMA-Cre;*Tgfbr2*$^{f/f}$ fibrotic kidneys, and morphometric analysis for relative interstitial fibrosis and tubular atrophy. (**h**) Immunolabeling and quantitative analysis for F4/80^{+} macrophages in αSMA-Cre;*Tgfbr2*$^{f/f}$ non-fibrotic (control) and WT and αSMA-Cre;*Tgfbr2*$^{f/f}$ fibrotic kidneys. AU: Arbitrary Units. DAPI(blue): nuclei. Scale bar: 50 μm. Data is presented as mean ± s.e.m. t-test, *P < 0.05.

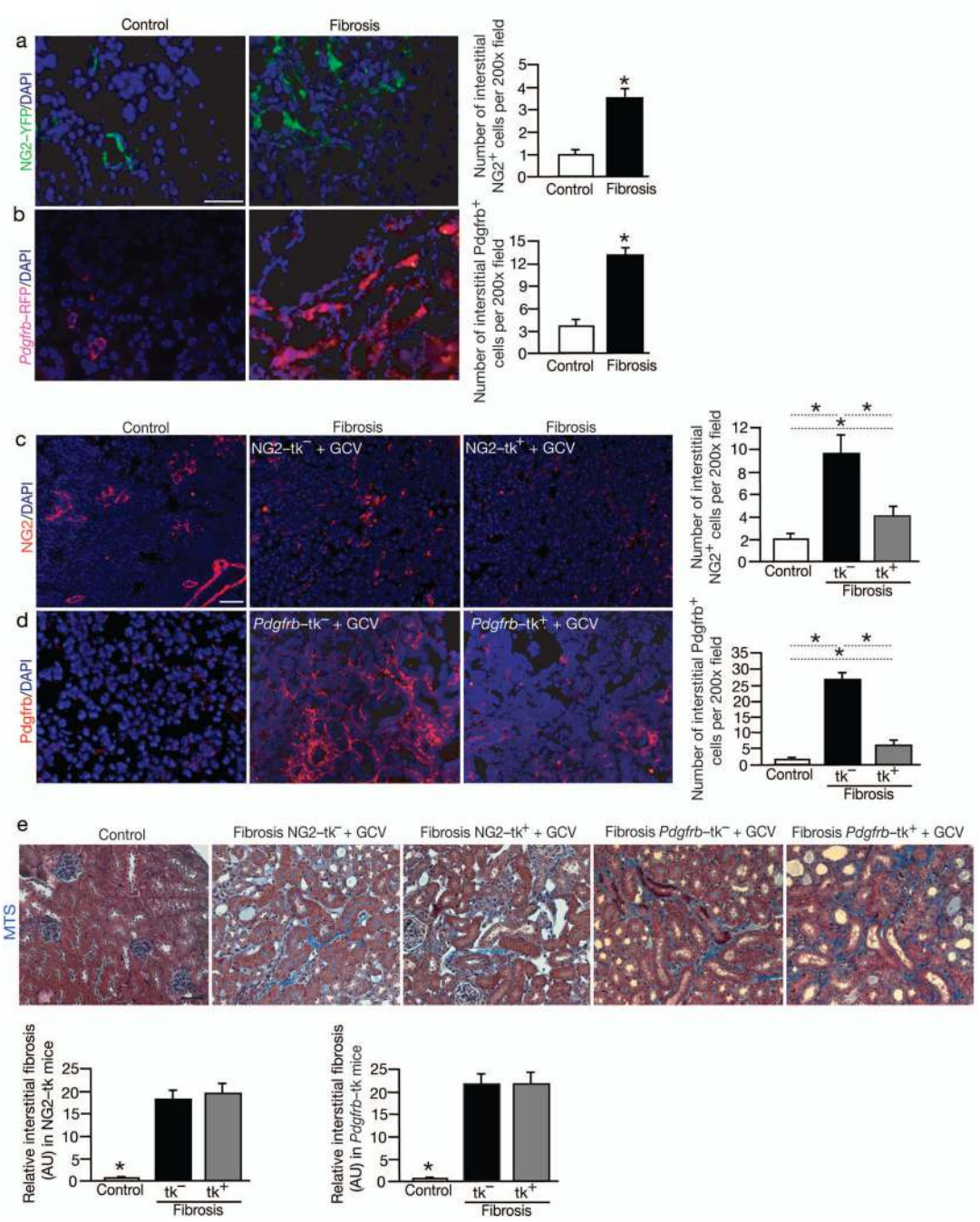

Fig. 4. NG2$^+$ and Pdgfrb$^+$ pericytes accumulate in the interstitium but do not functionally contribute to fibrosis

(**a**) Visualization and quantitation of NG2-YFP$^+$ cells in non-fibrotic contralateral (Control, $n = 5$) and fibrotic mouse kidneys from NG2-YFP transgenic mice ($n = 5$). (**b**) Visualization and quantitation of *Pdgfrb*-RFP$^+$ cells in non-fibrotic contralateral (Control, $n = 5$) and fibrotic mouse kidneys from *Pdgfrb*-RFP transgenic mice ($n = 5$). (**c**) Immunolabeling for NG2 and related quantitative analyses in non-fibrotic contralateral (Control, $n = 5$) and fibrotic kidneys from littermate WT (NG2-tk$^-$, $n = 5$) and NG2-tk$^+$ ($n = 5$) mice. (**d**)

Immunolabeling for Pdgfrb and related quantitative analyses in non-fibrotic contralateral (Control, $n = 5$) and fibrotic kidneys from littermate WT (*Pdgfrb*-tk^{-}, $n = 5$) and *Pdgfrb*-tk^{+} ($n = 5$) mice treated with GCV. (**e**) Representative Masson Trichrome staining (MTS) of non-fibrotic contralateral kidney (Control) and fibrotic kidney (Day 10 post UUO) of indicated experimental groups and respective morphometric analyses. AU: Arbitrary Units. DAPI(blue): nuclei. Scale bar: 50 μm. Data is presented as mean ± s.e.m. *t*-test, $^{*}P < 0.05$.

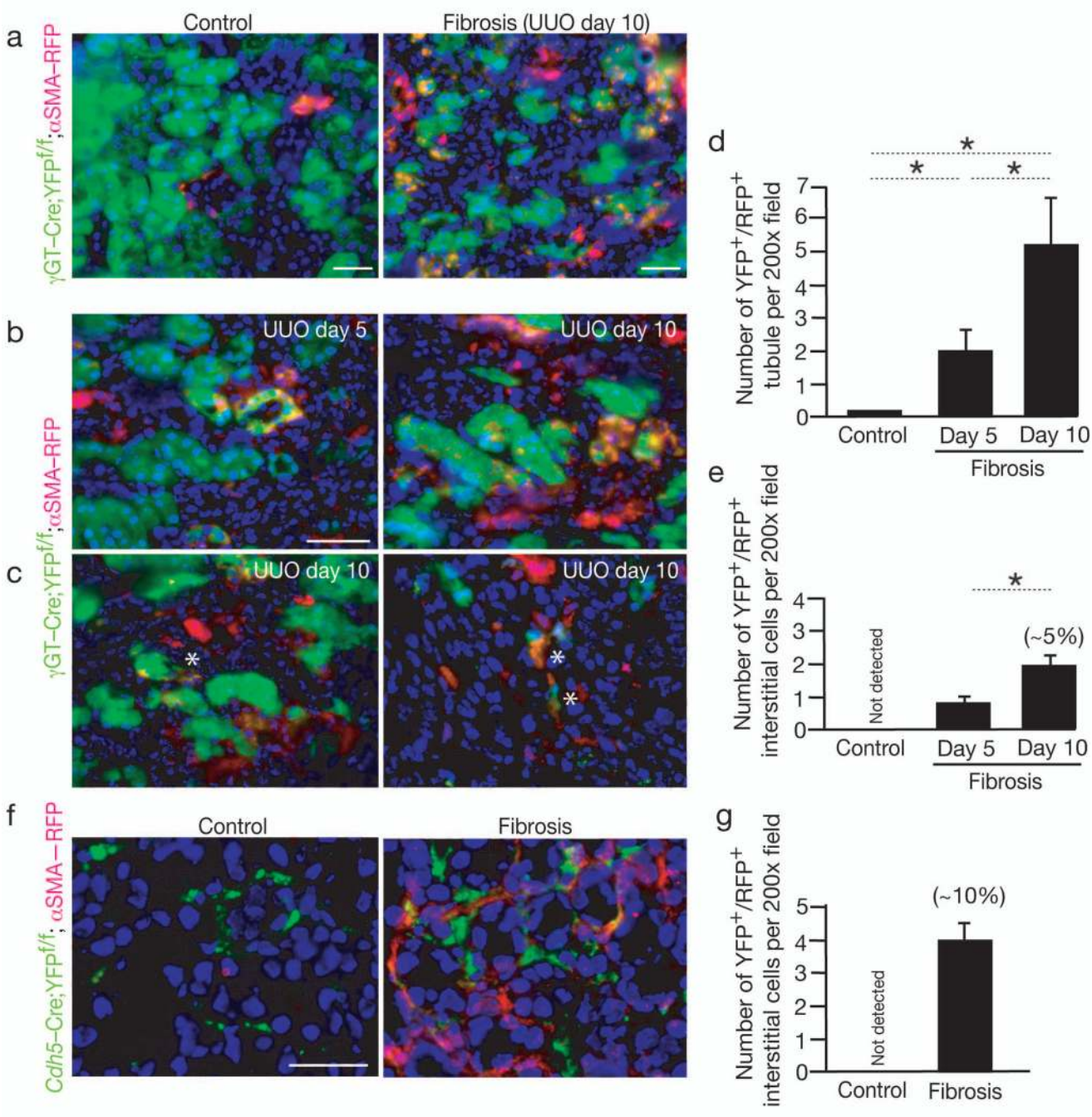

Fig. 5. Endothelial to Mesenchymal Transition contributes to myofibroblasts in fibrosis

(**a**) Representative imaging of healthy and fibrotic kidney (Day 10 post UUO) from γGT-Cre;YFP$^{f/f}$;αSMA-RFP mice: proximal tubules are green (YFP), interstitial myofibroblasts are red (RFP). (**b–c**) Higher magnification images of fibrotic kidney from γGT-Cre;YFP$^{f/f}$;αSMA-RFP mice at day 5 post UUO (n = 3), and at day 10 post UUO (n = 5). A star (*) indicates (**c**, left panel) a double positive (YFP$^+$/RFP$^+$) epithelial cells departing from the tubular basement membrane, and (**c**, right panel) interstitial double positive (YFP$^+$/RFP$^+$) myofibroblasts. (**d–e**) Quantitation of double positive tubules (**d**) and

interstitial myofibroblasts (**e**) in γGT-Cre;YFP$^{f/f}$;αSMA-RFP mice: non-fibrotic (Control) kidneys and fibrotic kidneys at day 5 and day 10 post UUO. The percentage listed is based on the observed total number of αSMA^{+} interstitial cells on day 10 post UUO. (**f**) Representative imaging of healthy contralateral kidney (Control, $n = 5$) and fibrotic (Day 10 post UUO, $n = 5$) from *Cdh5*-Cre;YFP$^{f/f}$;αSMA-RFP mice and (**g**) quantitation of double positive interstitial myofibroblasts. The percentage listed is based on the observed total number of αSMA^{+} interstitial cells on day 10 post UUO. DAPI(blue): nuclei. Scale bar: 50 μm. Data is presented as mean ± s.e.m. *t*-test, $^{*}P < 0.05$.